Continuous plating/stripping behavior of solid-state lithium metal anode in a 3D ion-conductive framework

Chunpeng Yang[a,1], Lei Zhang[a,1], Boyang Liu[a], Shaomao Xu[a], Tanner Hamann[a], Dennis McOwen[a], Jiaqi Dai[a], Wei Luo[a], Yunhui Gong[a], Eric D. Wachsman[a,2], and Liangbing Hu[a,2]

[a]Department of Materials Science and Engineering, University of Maryland, College Park, MD 20742

Edited by Thomas E. Mallouk, The Pennsylvania State University, University Park, PA, and approved March 2, 2018 (received for review November 20, 2017)

The increasing demands for efficient and clean energy-storage systems have spurred the development of Li metal batteries, which possess attractively high energy densities. For practical application of Li metal batteries, it is vital to resolve the intrinsic problems of Li metal anodes, i.e., the formation of Li dendrites, interfacial instability, and huge volume changes during cycling. Utilization of solid-state electrolytes for Li metal anodes is a promising approach to address those issues. In this study, we use a 3D garnet-type ion-conductive framework as a host for the Li metal anode and study the plating and stripping behaviors of the Li metal anode within the solid ion-conductive host. We show that with a solid-state ion-conductive framework and a planar current collector at the bottom, Li is plated from the bottom and rises during deposition, away from the separator layer and free from electrolyte penetration and short circuit. Owing to the solid-state deposition property, Li grows smoothly in the pores of the garnet host without forming Li dendrites. The dendrite-free deposition and continuous rise/fall of Li metal during plating/stripping in the 3D ion-conductive host promise a safe and durable Li metal anode. The solid-state Li anode shows stable cycling at 0.5 mA cm^{-2} for 300 h with a small overpotential, showing a significant improvement compared with reported Li anodes with ceramic electrolytes. By fundamentally eliminating the dendrite issue, the solid Li metal anode shows a great potential to build safe and reliable Li metal batteries.

lithium metal anode | solid-state electrolytes | 3D ion-conductive host | garnet electrolyte | dendrite-free

Developing energy-storage systems with high energy density as well as safety has attracted tremendous research interest in various electrochemical energy-storage devices. Lithium (Li) metal batteries have been widely considered as promising candidates for next-generation energy storage owing to their extremely high theoretical energy densities (e.g., 2,600 Wh kg^{-1} in Li-S battery and 3,500 Wh kg^{-1} in Li-air battery) (1, 2). However, the application of Li metal anodes has long been hindered by the safety hazard because of the Li dendrite growth and potential short circuit (3–6). It is imperative to build safe and dendrite-free Li metal anodes for the development of high-energy-density Li batteries. Current studies on Li metal anodes are mainly focused on improving the Li anodes with liquid electrolytes. Multiple effective approaches have been reported to improve the Li anodes, such as constraining Li metal in porous materials (7–10), creating protective layers for stabilizing the Li–electrolyte interface (11–15), and modifying the organic electrolytes (16–18). However, because of the intrinsic high reactivity of Li metal and dendrite-formation behavior of Li in liquid electrolytes, as well as the flammability and leakage of most organic electrolytes, the performance and safety of Li metal anodes still face great challenges (19).

Solid batteries are expected to fundamentally eliminate the safety concerns of Li metal anodes. Solid-state electrolytes, especially ceramic Li-ion conductors, show exceptional ability to inhibit the formation of Li dendrites and preclude the short-circuit hazard, and are nonflammable and nonleaking (20, 21). The problems of solid-state electrolytes lie in their relatively low ionic conductivities, which have been greatly improved recently, and the interface contact between the electrolyte and the electrode (22–25). For solid-state Li metal anodes, the lithiophobicity of the ceramic Li-ion conductors has resulted in poor interface contact and huge impedance. Therefore, many studies have been devoted to improving the Li–electrolyte interface by adding polymeric interlayers, coating lithiophilic layers, and the surface chemistry control method (26–33). Nevertheless, due to the inevitable existence of grain boundaries in the solid-state electrolyte, Li could still form dendrites and penetrate through the electrolyte, resulting in a short circuit (32, 34, 35). What is worse, drastic volume change during Li plating and stripping could further deteriorate the interface contact between the solid electrolyte and Li anode, increasing the impedance during cycling. The poor solid interface contact and volume change of Li anode during cycling have significantly limited the applicable capacity in previous research of Li metal anodes with ceramic electrolytes (26–33).

Herein, we demonstrate a safe Li metal anode by hosting Li metal in a 3D solid-state Li-ion-conductive host with a bottom-coated current collector. By cycling the Li anode within the 3D solid-state ion-conductive host, we investigate its plating/stripping behavior and demonstrate a safe and dendrite-free solid Li metal anode. As shown in Fig. 1*A*, the ion-conductive host consists of a dense layer as the separator and two porous layers for hosting

Significance

Solid-state lithium metal anode possesses great promise owing to its high energy density and improved safety. This work introduces a strategy for constructing a 3D Li metal anode, which is hosted in a solid-state ion-conducting host and shows a safe and dendrite-free plating/stripping behavior. The host is based on a garnet-type ion-conductive framework and a bottom-deposited Cu current collector. The Li anode is plated within the solid garnet framework from the bottom Cu layer and shows a dendrite-free deposition behavior, effectively averting the dendrite penetration issue. Owing to the 3D ion-conductive host, the volume change and interface contact problem of the Li anode have been significantly mitigated, realizing a high-capacity and safe Li metal anode for solid-state high-energy-density batteries.

Author contributions: C.Y., E.D.W., and L.H. designed research; C.Y., L.Z., B.L., S.X., T.H., and D.M. performed research; C.Y., L.Z., B.L., S.X., T.H., D.M., J.D., W.L., Y.G., E.D.W., and L.H. analyzed data; and C.Y., L.Z., E.D.W., and L.H. wrote the paper.

The authors declare no conflict of interest.

This article is a PNAS Direct Submission.

[1]C.Y. and L.Z. contributed equally to this work.

[2]To whom correspondence may be addressed. Email: ewach@umd.edu or binghu@umd.edu.

This article contains supporting information online at www.pnas.org/lookup/suppl/doi:10.1073/pnas.1719758115/-/DCSupplemental.

Published online March 26, 2018.

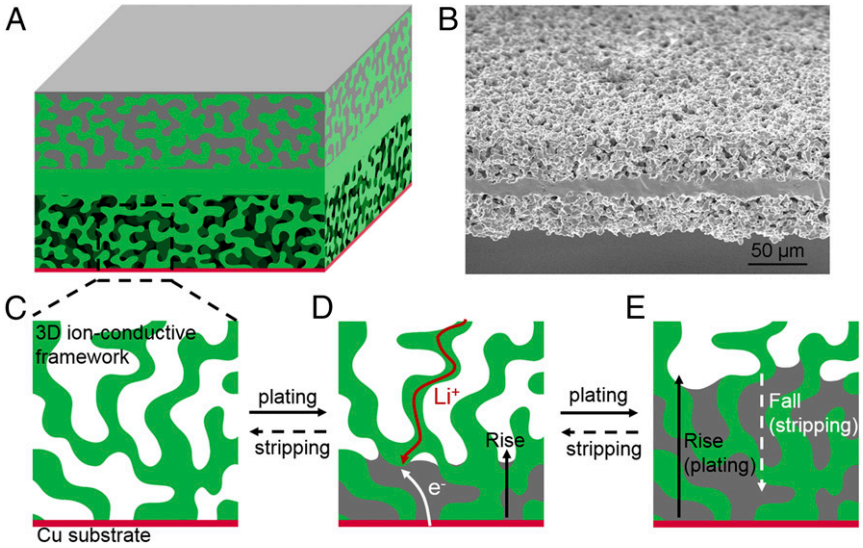

Fig. 1. Schematic for the process of Li plating and stripping in the 3D Li-ion-conductive host. (*A*) Schematic of the 3D ion-conductive host for studying Li-ion plating/stripping, where the upper layer is filled with the Li source and the lower layer is empty with Cu deposited on the bottom. (*B*) Side-view SEM image of the pristine 3D ion-conductive host. 2D local schematic for (*C*) the lower layer of the pristine empty host without Li, (*D*) Li deposited in the 3D ion-conductive host from the bottom current collector, and (*E*) more Li deposited and grown in the 3D host.

active materials and Li metal. The 3D ion-conductive framework was fabricated by using a $Li_7La_{2.75}Ca_{0.25}Zr_{1.75}Nb_{0.25}O_{12}$ (LLCZN) garnet-type Li-ion conductor (hereinafter, garnet) with a porous–dense–porous structure. Garnet-type Li-ion conductor is a promising solid-state electrolyte because of its excellent ionic conductivity, broad electrochemical stability window, and chemical stability (36, 37). A side-view scanning electron microscope (SEM) image of the garnet host is shown in Fig. 1*B*. The upper layer is filled with the Li source (Li metal in this study), the bottom layer is empty with a thin layer of Cu as the current collector, and the middle dense layer serves as a separator. As illustrated in Fig. 1 *C*–*E*, this structure enables Li deposition only from the bottom, where Li ions from the garnet skeleton gain electrons from the Cu (or Li deposited on Cu). With more Li deposited, the front of the Li-filled layer rises from the bottom Cu substrate within the 3D framework. Subsequent stripping leads to the fall of the Li metal. As plating/stripping of Li results in the rise/fall of the anode in the host structure and always away from the separator layer, internal short circuits caused by Li penetration are further averted. Moreover, since Li metal in the ion-conductive host is reduced from solid-state Li ions, Li is plated within the voids of the 3D framework without forming dendrites, in sharp contrast with Li hosts in liquid electrolytes. This Li metal anode that rises and falls in the solid ion-conductive framework opens an approach to building safe and durable Li metal batteries.

Results and Discussion

The porous–dense–porous garnet framework was synthesized by a tape-casting method (38). The cross-sectional view of the 3D garnet framework is shown in Fig. 2*A*. Same as the schematic in Fig. 1*A*, the garnet framework has a dense separating layer and two porous layers. The separating layer is 28 μm and each porous layer is ∼50 μm. By adjusting the garnet tapes, the thickness of the porous garnet layer is adjustable (20–150 μm) and its porosity is ∼50%, thus providing appropriate room for hosting active materials of various capacities. As confirmed by the X-ray diffraction (XRD) profiles in Fig. 2*B*, the 3D garnet shows a well-crystalline structure, coincident with the cubic-phase garnet $Li_5La_3Nb_2O_{12}$. As shown in the electrochemical impedance spectrum (EIS) in *SI Appendix*, Fig. S1, the garnet has a high ionic conductivity of 3×10^{-4} S cm^{-1} at room temperature (see *SI Appendix*, Fig. S1 for the ionic conductivity calculation using a dense garnet pellet), which facilitates the solid-state transport of Li ions.

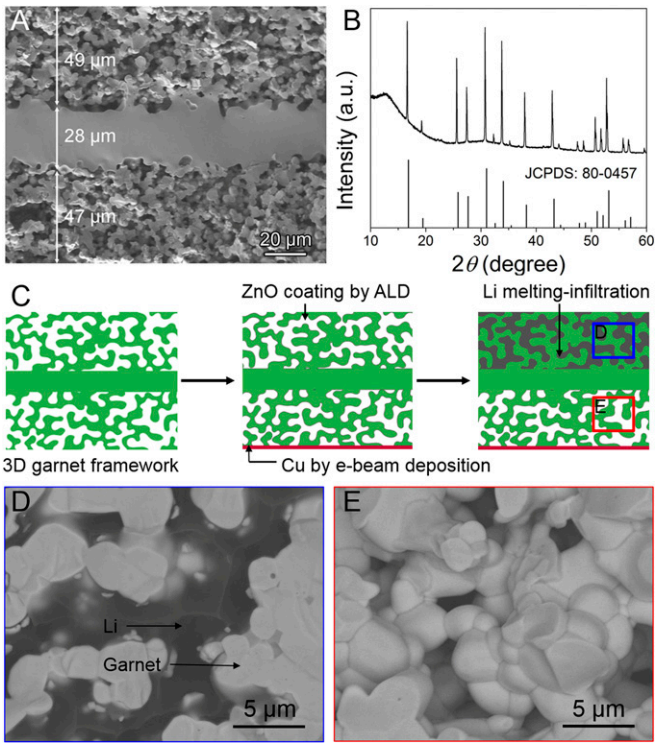

Fig. 2. Cell assembly for the solid-state Li metal anode study in a 3D garnet host. (*A*) Cross-sectional SEM image of the 3D garnet host. (*B*) XRD pattern of the 3D porous LLCZN pellet in comparison with standard cubic-phase $Li_5La_3Nb_2O_{12}$ (Joint Committee on Powder Diffraction Standards 80–0457). (*C*) Schematic showing the procedures to fill the upper layer of the porous garnet host with molten Li. SEM images of (*D*) the upper layer filled with Li metal by melt infiltration, where Li is dark color and garnet is bright as indicated by the arrows, and (*E*) the lower layer of porous garnet without Li infiltration, which is reserved for electrochemical Li deposition.

To conduct electrons, a thin layer of Cu (~200 nm) was deposited at the bottom of the 3D garnet by e-beam evaporation. As shown in the SEM image of the bottom layer and corresponding elemental mapping of Cu by energy-dispersive X-ray spectroscopy (EDX) (*SI Appendix*, Fig. S2), Cu was uniformly coated at the bottom of the garnet skeleton. Due to the directional deposition by an e-beam evaporation technique, Cu was not found inside the porous layer and served only as a current collector. The Cu current collector deposited on garnet framework significantly reduces the interfacial resistance in the cell (see EIS in *SI Appendix*, Fig. S3). The upper porous layer can be filled with cathode materials for assembly of full cells in practical uses. To study the Li plating/stripping behavior in the 3D ion-conductive host, we filled the upper porous garnet layer with Li metal as the Li source. Li was infiltrated into the upper porous layer by a melt-infiltration method, which is schematically presented in Fig. 2*C*. The upper layer of the porous garnet host was first coated with ZnO of ~50 nm by atomic layer deposition (ALD) to improve the wetting property of the garnet with molten Li (30). A thin Li foil was melted on top of the garnet pellet and infused into the pores of the upper layer by capillarity. The upper layer filled with Li can be clearly observed by SEM image of backscattered electrons (Fig. 2*D*), where the bright area indicates the garnet framework with heavy atoms (La, Zr, etc.) and the dark area indicates the infiltrated Li. The molten Li did not diffuse through the separating layer and the bottom porous layer remained empty, which is evidenced by the SEM image in Fig. 2*E* and the large-area cross-sectional SEM image in *SI Appendix*, Fig. S4. Therefore, the garnet framework is an excellent solid host structure for Li anode with a dense separating layer that blocks Li from penetration.

Using the empty porous garnet framework with the Cu substrate, we systematically studied the plating/stripping behavior of Li metal in the 3D garnet host. The voltage profile of Li plating into the garnet host at 0.5 mA cm^{-2} is shown in Fig. 3*A*. During Li deposition, the Li ions migrate through the 3D garnet skeleton while the electrons transport from the Cu current collector (and already-deposited Li metal). Since all electrons come from the bottom current collector, Li metal is always deposited from the bottom and rises with further Li deposition, as depicted in Fig. 3*B*. The deposition of Li on the bottom Cu leads to a significant reduction of the interface resistance of the cell (*SI Appendix*, Fig. S5). Fig. 3 *C* and *D* shows two regions of the cross-section of the garnet host (as indicated in Fig. 3*B*) after Li deposition. After Li plating, the garnet host near the separating layer in Fig. 3*C* remains empty while the bottom part is electrochemically deposited with Li metal (dark regions in the pores of the garnet framework). Although the Li cannot be detected by EDX, the SEM image of the garnet framework after Li plating (Fig. 3*E*) and corresponding La elemental mapping in garnet (Fig. 3*F*) clearly indicate that the Li metal is filled in the voids of the garnet skeleton, covering the signal of La in the EDX mapping. The bottom Cu plays a key role in providing electronic access; without the bottom Cu layer, Li can plate outside of the framework (*SI Appendix*, Fig. S6). The SEM images and EDX mapping confirm the deposition behavior of the Li metal anode illustrated in Fig. 3*B*, i.e., Li is plated initially on the bottom Cu layer away from the separating layer, averting possible dendrite penetration and short circuit.

The plating and stripping behavior of the Li metal anode in the 3D garnet host was further studied by plating Li with different areal capacities. As demonstrated above, plating of Li within the solid-state garnet framework starts from the electron-conductive Cu layer. During further Li deposition, Li metal grows continuously on the previous Li, where Li ions from the garnet framework gain electrons from the already-deposited Li metal and Cu substrate. This deposition behavior leads to the rise of Li in the host during Li deposition as depicted in Fig. 4*A*.

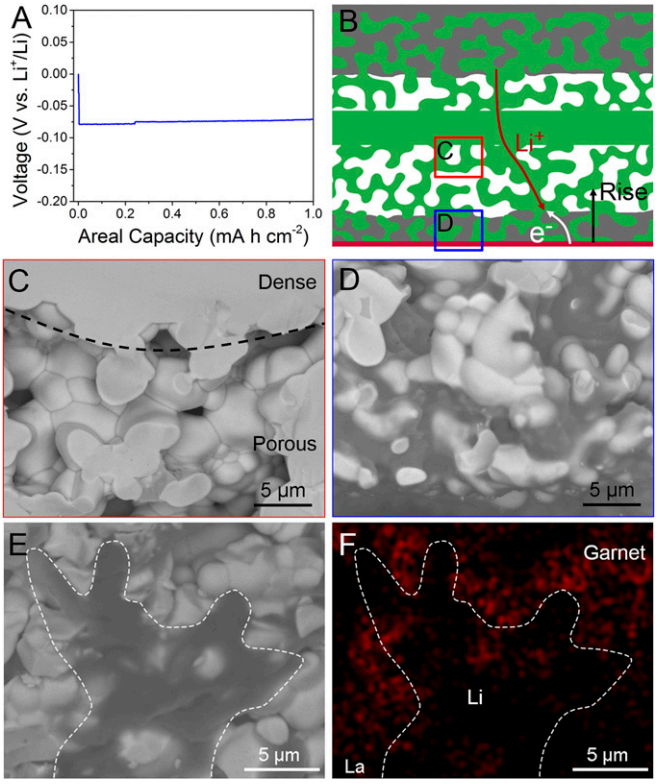

Fig. 3. Li deposition behavior in the 3D garnet host. (*A*) Voltage profile of Li plating within the porous garnet framework onto the bottom Cu layer at 0.5 mA cm^{-2}. (*B*) Schematic of Li growth in the 3D garnet framework with Cu current collector and transfer of Li ions and electrons. Cross-sectional SEM images of 3D garnet host after deposition of Li metal in two regions indicated in *B*: (*C*) near the dense separating layer, where the pores of the garnet host remain empty without Li deposition, (*D*) bottom region with Cu current collector, where the garnet host is deposited with Li metal. (*E*) Cross-sectional SEM image and (*F*) corresponding elemental distribution of La in the Li-deposited 3D garnet host.

The SEM image (Fig. 4*B*) of Li metal deposited in the garnet host for 2 mA h cm^2 displays a consistent result. Li is plated in the lower layer of the garnet host and shows a rising growth profile. The Li filled in the garnet host is ~50 μm, mainly grown on the bottom Cu substrate, while leaving the separator-adjacent garnet host empty. Li metal of 3 mA h cm^{-2} also shows a coincident result with a Li deposition thickness of ~70 μm (*SI Appendix*, Fig. S7). The thicknesses of Li deposited within the garnet host with different capacities of Li are summarized in Fig. 4*C*. The thickness of the hosted Li metal anode shows an approximately linear relationship to the areal capacity, which indicates that Li roughly rises from the bottom current collector during plating. After stripping the Li in the garnet host, it is found that only residual Li remains on the bottom of the host (*SI Appendix*, Fig. S8) and Li height "falls" to nearly 0. This unique plating/stripping behavior guarantees safe Li metal anodes as Li metal is initially deposited on the bottom current collector far from the separator and fills the preserved pores in the ion-conductive host, avoiding the interface contact problem in planar solid electrolytes.

Another prominent advantage of the proposed 3D Li metal anode enabled by the solid-state ion-conductive host is that the Li dendrite problem is significantly eliminated. As shown in Fig. 4*D*, Li metal deposited in the porous garnet at 0.05 mA cm^{-2} shows an extremely dense and smooth morphology, without any dendritic Li, which is a major issue in liquid electrolyte Li metal anodes. The smooth and dense deposition of Li metal results

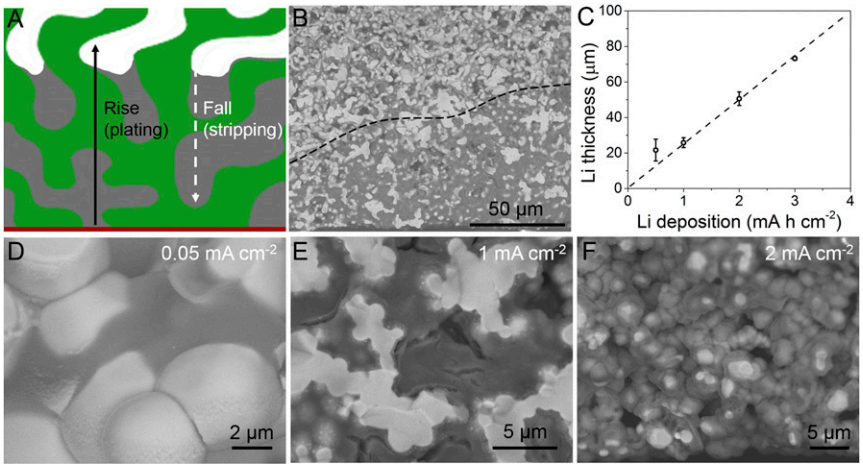

Fig. 4. Li plating/stripping behavior in the garnet framework. (*A*) Schematic of Li rise/fall within the garnet framework during plating/stripping. (*B*) SEM image of 2 mA h cm^{-2} of Li deposited in the garnet framework. (*C*) Evolution of Li deposition thickness with the areal capacity of deposited Li. Cross-sectional SEM images of Li deposited in garnet framework at different current densities: (*D*) 0.05 mA cm^{-2}, (*E*) 1 mA cm^{-2}, and (*F*) 2 mA cm^{-2}.

from a balance of Li ions transferred from the garnet framework and the electrons from the Cu current collector. At increased current densities, the morphology of deposited Li changes, but the dendritic Li is eliminated. As shown by the SEM images, Li anodes deposited at 0.5 mA cm^{-2} (Fig. 3*D*), 1 mA cm^{-2} (Fig. 4*E*), and 2 mA cm^{-2} (Fig. 4*F*) do not form any dendrites,

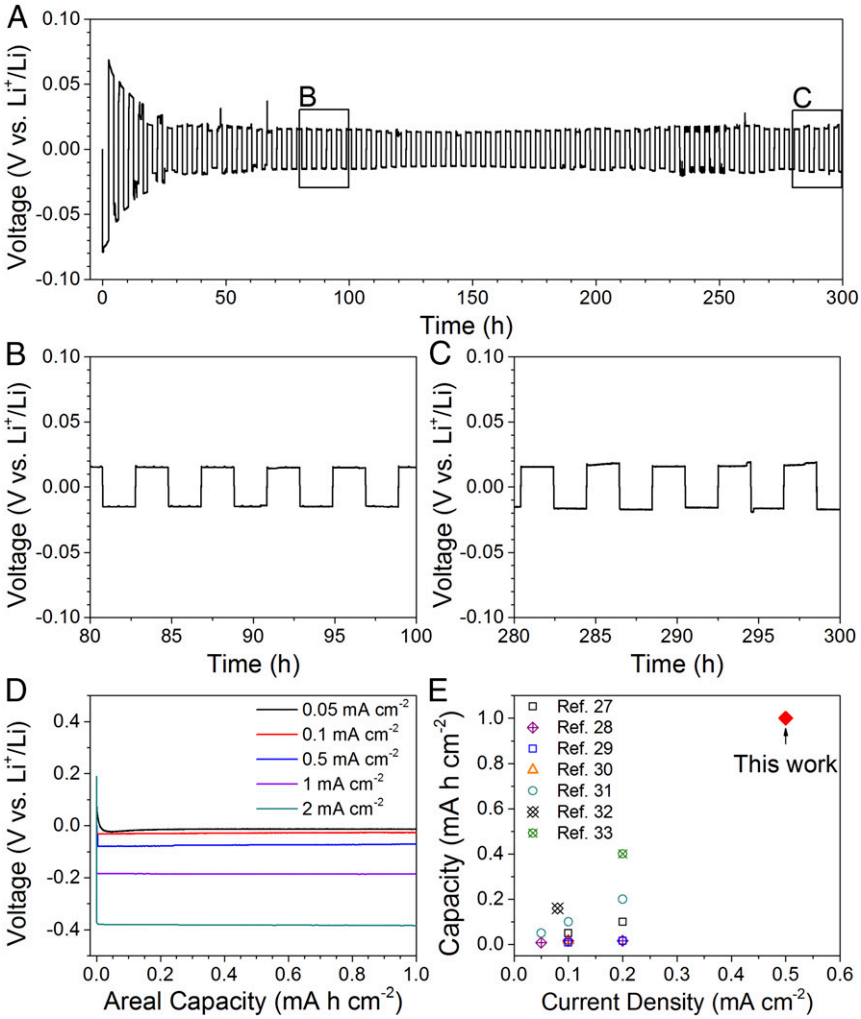

Fig. 5. Electrochemical properties of Li plating/stripping within the garnet host. (*A*) Discharge/charge voltage profiles of the Li cycling in the garnet host at 0.5 mA cm^{-2} and local view of voltage profiles at (*B*) 80–100 h and (*C*) 280–300 h. (*D*) Voltage profiles of Li plating at different current densities in the garnet host. (*E*) Comparison of the cyclable areal capacity and current density of Li metal anodes in this work and previous publications with oxide-based solid-state electrolytes (27–33).

although Li deposited at higher current densities is not as dense as that deposited at 0.05 mA cm^{-2}. The dendrite-free Li anode in the garnet host should be attributed to the solid-state Li deposition, which contrasts starkly with that in liquid electrolytes. In liquid electrolytes, Li ions are ubiquitous and Li dendrites are inevitable. As a control experiment, even if 10 μL of liquid electrolyte was added to the porous garnet framework, Li dendrites were observed and Li was not constrained in the framework after plating (*SI Appendix*, Fig. S9). Using the solid-state garnet host, the Li ions diffuse only through the ionic-conductive skeleton and Li is deposited only at the interface of ion conductor and electron conductor, without forming dendritic morphology.

The cyclability of the solid-state Li metal anode in 3D ion-conductive host was further demonstrated by cycling the Li metal anode in the garnet framework at 0.5 mA cm^{-2}. As shown in cycling voltage profiles and zoom-in profiles in Fig. 5 *A*–*C*, the solid-state Li metal anode was cycled for 300 h at 0.5 mA cm^{-2} for an areal capacity of 1 mA h cm^{-2} each half cycle (1.5 mA h cm^{-2} for the initial plating). The voltage overpotential is gradually reduced from ∼80 to ∼20 mV during the first several cycles, indicating an improved interface contact of electron conductor (Li metal) and ion conductor (garnet framework) during initial cycles, which was demonstrated by EIS in *SI Appendix*, Fig. S5. The Li anode in the garnet host shows a stable plating/stripping voltage of ∼20 mV (Fig. 5 *B* and *C*) after the first several cycles and cycles for 300 h. The long-term cycling performance is associated with a high Coulombic efficiency (>100%; see discussion in *SI Appendix*, Fig. S10). Slightly excess Li in the anode (as we did in Fig. 5*A*) and the high Coulombic efficiency will greatly enhance the cycling performance. The stabilized overpotential of the solid-state Li metal anode is almost as small as that of the Li metal anode using liquid electrolytes, which should be attributed to the high ionic conductivity of the garnet-type ion conductor and the thin separating layer. The stable cycling performance results from the advantageous plating/stripping behavior of Li metal within the garnet host, in which the solid-state Li metal anode is free from dendritic Li and solid-state interface problems. Different current densities, from 0.05 to 2 mA cm^{-2}, were applied to plate Li into the garnet host on the Cu layer, of which discharge voltage profiles are shown in Fig. 5*D*. The solid-state Li metal anode can be plated for 1 mA h cm^{-2} at even 2 mA cm^{-2}, which has hardly been achieved in ceramic solid-state batteries.

In Fig. 5*E*, we compare the cycling capacities and current densities of Li metal anodes in this work with several publications using oxide-based solid-state electrolytes (27–33). The Li anode in the 3D garnet host shows a much higher capacity than previous studies using planar ceramic electrolytes. Hindered by the volume change at the anode–electrolyte interface during cycling, the previously reported solid-state Li anodes with ceramic electrolytes were generally limited to low capacities and small current densities (27–33). By depositing Li metal anode in the garnet host, the Li anode is exempt from most solid-solid interface problems and can thus safely cycle with increased capacities at higher current densities. We note that the rate capability of the Li anode with the ceramic solid-state electrolyte is still lower than that in liquid electrolytes. The solid-state Li anode generally shows a larger voltage polarization, especially during the initial cycles (80 mV at 0.5 mA cm^{-2}), than the Li anodes in liquid electrolytes (∼25 mV at 0.5 mA cm^{-2}). However, the incomparable advantage of the solid-state Li anode lies in the intrinsically safe deposition behavior, which improves not only the battery safety but also the cell cyclability. With further development of advanced ceramic electrolytes with enhanced ionic conductivity, the solid-state Li metal anode is expected to exhibit electrochemical performance comparable to that of Li metal anode with liquid electrolytes while fundamentally averting the safety issues in liquid electrolyte Li metal batteries. While the porous garnet framework in this work was filled with Li metal to investigate the Li plating/stripping behavior, the garnet framework with the porous–dense–porous structure is a superb host for high-energy-density batteries, with one porous layer accommodating the Li anode and the other for cathode materials such as sulfur (see the schematic of a projected solid-state Li-S battery in *SI Appendix*, Fig. S11 with the garnet framework). The Li content in the LLCZN electrolyte is 6.0% and the equivalent Li content in the cell (including Li in the electrolyte, excluding the cell package) is 10.1%. The energy density of the garnet-based solid-state Li-S battery is projected to reach 518.4 W h kg^{-1} or 1,210.1 W h L^{-1} (see calculation details in *SI Appendix*, Table S1), very promising for high-energy-density systems.

Conclusion

In summary, we have demonstrated a safe and dendrite-free Li metal anode in a solid-state 3D ion-conductive host. By depositing Li metal into the 3D garnet framework with Cu current collector at the bottom, Li metal is plated from the bottom of the 3D host away from the separating layer and gradually fills the garnet host. Since the Li is initially plated on the bottom current collector away from the separator, any possible penetration through the electrolyte can also be prevented. The solid-state depositing property of Li ions eliminates the dendritic morphology of Li metal anodes, which is inevitable with liquid electrolytes. Deposition of Li within the preserved pores of the garnet host effectively mitigates the volume change issue of Li anode during cycling and improves the electrolyte–anode interface contact. The solid Li metal anode in the garnet host exhibits an exceptional cycling stability. It can be cycled for 1 mA h cm^{-2} at 0.5 mA cm^{-2} for 300 h without dendrite-induced short circuit or significant overpotential. Benefiting from the 3D ion-conductive host, the solid Li anode can be cycled for 1 mA h cm^{-2}, which is much higher than most previous solid-state Li anodes based on oxide-based solid-state electrolytes and is comparable to Li anodes in liquid electrolyte batteries. The dendrite-free and safe depositing properties of the solid Li anode in the ion-conductive host introduce a strategy to build safe and durable high-energy metal batteries for next-generation energy storage.

Methods

Garnet Solid Electrolyte Fabrication. LLCZN powder was synthesized by conventional solid-state reaction. The starting materials were LiOH (99%; Alfa Aesar), La_2O_3 (99.9%; Alfa Aesar), $CaCO_3$ (99.9%; Sigma-Aldrich), ZrO_2 (99.9%; Alfa Aesar), and Nb_2O_5 (99.99%; Alfa Aesar). Stoichiometric amounts of the raw materials and 10% excess LiOH were mixed by ball-milling and calcined at 900 °C for 12 h.

Tape casting was used to fabricate the trilayer framework. LLCZN was mixed with fish oil, polyvinyl butyral, and butyl benzyl phthalate in toluene and isopropanol to prepare the slurry, which was cast by a doctor blade on Mylar sheet. Poly(methyl methacrylate) spheres were added as porogens in porous tape. The pore size of the porous layer can be controlled by the size of polymer-based pore formers and its content. Dense and porous layers were fabricated separately and then laminated into a trilayer tape. The thickness of each individual layer was well controlled. The tapes were laminated and hot-pressed to form a trilayer structure. Then it was sintered at 1,050 °C for 1 h to obtain the porous–dense–porous garnet framework.

Cell Assembly. The Cu layer deposited at the bottom of the garnet host was sputtered by an electron-beam physical vapor deposition on an Angstrom NexDep Ebeam Evaporator. The upper layer of the garnet host was coated with ZnO by ALD to increase its wettability with molten Li. The ALD deposition of ZnO was performed on Beneq TFS 500 at 150 °C for 150 cycles. Each cycle alternates reactions of diethyl zinc or water with the 3D garnet pellet. Li was then infiltrated into the host from top of the garnet pellet (without Cu deposition and with ZnO coating) by melt infiltration in an argon-filled glovebox. A fresh piece of Li foil was placed on the garnet host and was covered by stainless steel, which provided suitable pressure for Li infiltration into the garnet pores. The Li on garnet pellet was heated at

250 °C in an oven in the glovebox for 30 min, during which Li impregnated into the upper porous layer of the garnet host. The as-obtained porous garnet pellet with one side filled with Li and the other empty side deposited with Cu was used as a solid-state cell for electrochemical study.

Characterizations and Electrochemical Tests. To determine the crystal structure of the 3D garnet host, XRD was performed on a C2 Discover diffractometer (Bruker AXS) with a Cu Kα radiation source (λ = 1.54056 Å) at 40 kV and 40 mA. Morphology and elemental distribution of the garnet host with or without Li were observed on a Hitachi SU-70 SEM coupled with an EDX system by collecting secondary electrons and backscattered electrons.

Electrochemical tests were conducted on BioLogic VMP3 electrochemical systems connected to the assembled solid-state cells in the glovebox. The side of garnet host filled with Li was used as a counter/reference electrode while the other empty side deposited with Cu was used as a working electrode to study the behavior of Li metal plating/stripping. EIS was measured in the frequency range of 1 MHz to 0.1 Hz. Galvanostatic Li plating was performed at 0.05–2 mA cm^2 for a capacity of 1 mA cm^{-2}. Plating/stripping of Li metal with the garnet host was performed at 0.5 mA cm^{-2} for 1 mA h cm^{-2}.

ACKNOWLEDGMENTS. We acknowledge Maryland Nanocenter, and its AIMLab and FabLab. This work was supported by the US Department of Energy Advanced Research Projects Agency - Energy (Contract DE-AR0000384) and Office of Energy Efficiency and Renewable Energy (Contract DE-EE0006860).

1. Lin D, Liu Y, Cui Y (2017) Reviving the lithium metal anode for high-energy batteries. *Nat Nanotechnol* 12:194–206.
2. Bruce PG, Freunberger SA, Hardwick LJ, Tarascon JM (2011) Li-O_2 and Li-S batteries with high energy storage. *Nat Mater* 11:19–29.
3. Xu W, et al. (2014) Lithium metal anodes for rechargeable batteries. *Energy Environ Sci* 7:513–537.
4. Kim H, et al. (2013) Metallic anodes for next generation secondary batteries. *Chem Soc Rev* 42:9011–9034.
5. Cheng X-B, Zhang R, Zhao C-Z, Zhang Q (2017) Toward safe lithium metal anode in rechargeable batteries: A review. *Chem Rev* 117:10403–10473.
6. Wood KN, Noked M, Dasgupta NP (2017) Lithium metal anodes: Toward an improved understanding of coupled morphological, electrochemical, and mechanical behavior. *ACS Energy Lett* 2:664–672.
7. Liang Z, et al. (2016) Composite lithium metal anode by melt infusion of lithium into a 3D conducting scaffold with lithiophilic coating. *Proc Natl Acad Sci USA* 113: 2862–2867.
8. Yang C-P, Yin Y-X, Zhang S-F, Li N-W, Guo Y-G (2015) Accommodating lithium into 3D current collectors with a submicron skeleton towards long-life lithium metal anodes. *Nat Commun* 6:8058.
9. Zhang R, et al. (2017) Advanced micro/nanostructures for lithium metal anodes. *Adv Sci (Weinh)* 4:1600445.
10. Lin D, et al. (2017) Three-dimensional stable lithium metal anode with nanoscale lithium islands embedded in ionically conductive solid matrix. *Proc Natl Acad Sci USA* 114:4613–4618.
11. Zheng G, et al. (2014) Interconnected hollow carbon nanospheres for stable lithium metal anodes. *Nat Nanotechnol* 9:618–623.
12. Zhu B, et al. (2017) Poly(dimethylsiloxane) thin film as a stable interfacial layer for high-performance lithium-metal battery anodes. *Adv Mater* 29:1603755.
13. Cheng XB, et al. (2015) A review of solid electrolyte interphases on lithium metal anode. *Adv Sci (Weinh)* 3:1500213.
14. Kozen AC, et al. (2015) Next-generation lithium metal anode engineering via atomic layer deposition. *ACS Nano* 9:5884–5892.
15. Li NW, Yin YX, Yang CP, Guo YG (2016) An artificial solid electrolyte interphase layer for stable lithium metal anodes. *Adv Mater* 28:1853–1858.
16. Ding F, et al. (2013) Dendrite-free lithium deposition via self-healing electrostatic shield mechanism. *J Am Chem Soc* 135:4450–4456.
17. Lu Y, Tu Z, Archer LA (2014) Stable lithium electrodeposition in liquid and nanoporous solid electrolytes. *Nat Mater* 13:961–969.
18. Suo L, Hu Y-SS, Li H, Armand M, Chen L (2013) A new class of solvent-in-salt electrolyte for high-energy rechargeable metallic lithium batteries. *Nat Commun* 4:1481.
19. Yang C, Fu K, Zhang Y, Hitz E, Hu L (2017) Protected lithium-metal anodes in batteries: From liquid to solid. *Adv Mater* 29:1701169.
20. Janek J, Zeier WG (2016) A solid future for battery development. *Nat Energy* 1:16141.
21. Xin S, et al. (2017) Solid-state lithium metal batteries promoted by nanotechnology: Progress and prospects. *ACS Energy Lett* 2:1385–1394.
22. Manthiram A, Yu X, Wang S (2017) Lithium battery chemistries enabled by solid-state electrolytes. *Nat Rev Mater* 2:16103.
23. van den Broek J, Afyon S, Rupp JLM (2016) Interface-engineered all-solid-state Li-ion batteries based on garnet-type fast Li^+ conductors. *Adv Energy Mater* 6:1600736.
24. Zhu Y, He X, Mo Y (2015) Origin of outstanding stability in the lithium solid electrolyte materials: Insights from thermodynamic analyses based on first-principles calculations. *ACS Appl Mater Interfaces* 7:23685–23693.
25. Richards WD, Miara LJ, Wang Y, Kim JC, Ceder G (2016) Interface stability in solid-state batteries. *Chem Mater* 28:266–273.
26. Zhou W, et al. (2016) Plating a dendrite-free lithium anode with a polymer/ceramic/polymer sandwich electrolyte. *J Am Chem Soc* 138:9385–9388.
27. Han X, et al. (2017) Negating interfacial impedance in garnet-based solid-state Li metal batteries. *Nat Mater* 16:572–579.
28. Luo W, et al. (2016) Transition from superlithiophobicity to superlithiophilicity of garnet solid-state electrolyte. *J Am Chem Soc* 138:12258–12262.
29. Fu KK, et al. (2017) Toward garnet electrolyte-based Li metal batteries: An ultrathin, highly effective, artificial solid-state electrolyte/metallic Li interface. *Sci Adv* 3: e1601659.
30. Wang C, et al. (2017) Conformal, nanoscale ZnO surface modification of garnet-based solid-state electrolyte for lithium metal anodes. *Nano Lett* 17:565–571.
31. Li Y, et al. (2016) Mastering the interface for advanced all-solid-state lithium rechargeable batteries. *Proc Natl Acad Sci USA* 113:13313–13317.
32. Tsai CL, et al. (2016) $Li_7La_3Zr_2O_{12}$ interface modification for Li dendrite prevention. *ACS Appl Mater Interfaces* 8:10617–10626.
33. Sharafi A, et al. (2017) Surface chemistry mechanism of ultra-low interfacial resistance in the solid-state electrolyte $Li_7La_3Zr_2O_{12}$. *Chem Mater* 29:7961–7968.
34. Sudo R, et al. (2014) Interface behavior between garnet-type lithium-conducting solid electrolyte and lithium metal. *Solid State Ion* 262:151–154.
35. Ren Y, Shen Y, Lin Y, Nan C-W (2015) Direct observation of lithium dendrites inside garnet-type lithium-ion solid electrolyte. *Electrochem Commun* 57:27–30.
36. Thangadurai V, Narayanan S, Pinzaru D (2014) Garnet-type solid-state fast Li ion conductors for Li batteries: Critical review. *Chem Soc Rev* 43:4714–4727.
37. Murugan R, Thangadurai V, Weppner W (2007) Fast lithium ion conduction in garnet-type $Li_7La_3Zr_2O_{12}$. *Angew Chem Int Ed Engl* 46:7778–7781.
38. Fu K, et al. (2017) Three-dimensional bilayer garnet solid electrolyte based high energy density lithium metal-sulfur batteries. *Energy Environ Sci* 10:1568–1575.